ISSN 1343-2230
CNS-REP-39
October, 2001

CNS Report

Low-Energy RI Beam Separator CRIB

T. Teranishi, S. Kubono, Y. Yanagisawa, S. Shimoura,
Y. Mizoi, M. Notani, S. Michimasa, K. Ue, S. Watanabe,
N. Yamazaki, M. Oshiro, T. Kishida and S. Kato

* *Presented at International Workshop on Production of Radioactive Ion Beams (PRORIB-2001), Feb. 12-17, 2001, Puri, India*

Center for Nuclear Study (CNS)

Graduate School of Science, the University of Tokyo
Wako Branch at RIKEN, Hirosawa 2-1, Saitama 351-0198, Japan
Correspondence: cnsoffice@cns.s.u-tokyo.ac.jp

Low-Energy RI Beam Separator CRIB

T. Teranishi[1*], S. Kubono[1], Y. Yanagisawa[2], S. Shimoura[1], Y. Mizoi[2], M. Notani[1], S. Michimasa[1], K. Ue[1], S. Watanabe[1], N. Yamazaki[1], M. Oshiro[1], T. Kishida[2] and S. Kato[3]

[1]*Center for Nuclear Study (CNS), University of Tokyo, RIKEN campus, Hirosawa 2-1, Wako, Saitama, 351-0198 Japan*

[2]*RIKEN (The Institute of Physical and Chemical Research), Hirosawa 2-1, Wako, Saitama, 351-0198 Japan*

[3]*Physics Department, Yamagata University, Yamagata, 990-8560 Japan*

[*]*e-mail: teranisi@cns.s.u-tokyo.ac.jp*

Abstract

This paper introduces the low-energy radio-isotope (RI) beam separator CRIB, which has been constructed at Center for Nuclear Study (CNS), University of Tokyo, and is almost ready for operation. The technique of RI beam production and separation used for CRIB is discussed. An experimental project of elastic resonance scattering by using CRIB is also briefly described.

I. INTRODUCTION

RI beams at a low-energy region (1–10 MeV/u) are useful for spectroscopy of unstable nuclei and study of nuclear reactions for nuclear astrophysics. To produce RI beams efficiently at this energy region, we have installed an in-flight RI-beam separator CRIB at the RIKEN Accelerator Research Facility (RARF) under the CNS-RIKEN joint project. Many facilities have already developed in-flight type RI beam separators utilizing projectile fragmentation reactions at several tens MeV/nucleon. These fragment separators are not optimized for low-energy beams and instead the ISOL method has often been applied to

the production of low-energy RI beams. The ISOL method has an advantage of small beam emittance. However, it sometimes requires high technology for ion-source/production-target and therefore number of available nuclides is rather limited.

We have chosen at low-energy an in-flight method, which was not considered so seriously before because the effective target thickness usable for RI beam production is too thin to get a high intensity. However, recent development of ion source technology for heavy ions enables one to produce reasonably high intensity primary beams which overcome the disadvantage of thin target. We mainly use two-body reactions such as (p,n) reactions in inverse kinematics. In this case, emittances of the RI beams can be small and comparable to the acceptance of our separator. Thus, our method is one of the effective solutions of low-energy RI beam production.

Primary beams for CRIB are provided by the AVF cyclotron ($K = 70$), which can accelerate a variety of heavy-ion beams ($A < 40$) with energies up to about 10 MeV/nucleon and intensities as high as 100 pnA (several hundreds pnA for $A < 20$ ions). The cyclotron is one of the two injector accelerators for the main ring-cyclotron ($K = 540$) at RARF. When the other injector, a liniac, is being used for the ring cyclotron, the AVF cyclotron can be operated for CRIB in parallel. A beam line from AVF directly to CRIB is provided for the parallel operation.

The most of magnets used for CRIB were originally built for the polarization spectrograph DUMAS [1] nearly twenty years ago. The design of CRIB was based on these magnets and a lot of modifications and extensions were made for RI beam separation.

II. CHARACTERISTIC OF CRIB

Figure 1 shows the layout of CRIB. A low-energy RI beam is produced at the target position F0 as an ejectile of reaction induced by a low-energy heavy-ion beam from the AVF cyclotron. The RI particles are then collected and separated from other reaction products by the CRIB. The CRIB separator consists of two major components, a magnetic separator

with dispersive and achromatic focal planes (F1 and F2, respectively) and a Wien filter which is under construction after F2.

A. Production Targets at F0

Usually, production targets are set inside of a small chamber at F0. Two types of target, thin foil and gas cell, is applicable to the F0 chamber. For example, a thin foil of CH_2 may be used for (p,n) reactions. However, the CH_2 foil is not usable with high intensity primary beams because the foil is not tolerant of heat. Instead, gas targets like H_2 or CH_4 should be used to produce reasonably high intensity secondary beams. The target gas is confined in a small cell with entrance and exit windows made of Havor foils.

In addition to the F0 target chamber, we have another target chamber for a window-less gas target with differential pumping systems. The window-less gas target is useful when the primary beam intensity needs to be extremely high and window foils are not usable because of heat, and also useful when the energy losses at window foils are too large for low energy beams.

The window-less gas target system is a blow-in type developed by Sagara et al. [2]. The target gas is blown into the central region of the target cell from both the upstream and the downstream ends. The length of the target cell is 10 cm along the beam axis. There are four outer vacuum chambers of increasing sizes with differential pumping systems as shown in Fig. 1 of Ref. [2]. All four of the upstream apertures are 6 mm in diameter to ensure that they are not touched by the incoming ion beams. The diameters of the down stream apertures are 6, 6, 8 and 10 mm, respectively, from the target cell, taking into account an emittance of reaction products.

A pressure of 6×10^{-6} Torr could be maintained in the outermost vacuum chamber with a target gas pressure of 50 Torr for N_2. The first stage pump is a vane type low-vacuum pump with a pumping speed of 1020 m^3/h, which takes most of the target gas leaking out of the 6 mm diameter apertures of the target cell. The next surrounding vacuum chamber is equipped

with a pump of the same pumping speed. The last two outer vacuum chambers are equipped with turbomolecular pumps with a pumping speeds of 1450 and 550 l/s, respectively.

The target gas can be recirculated to prevent contamination of the environment by reaction product activities. This recirculation system dramatically reduces gas consumption, which is less than 1 m^3 at 1 atmosphere for two days of operation.

B. Magnetic Spectrometer

The magnetic separator consists of two dipole magnets (D1 and D2) and four quadrupole magnets (Q1, Q2, M3 and Q3) in a sequence of F0-Q1-D1-Q2-F1-D2-M3-Q3-F2, where F0, F1 and F2 represent the target point, the first and second focal planes, respectively (see Fig. 1). Figure 2 shows a result of first-order optics calculation for CRIB by using the code TRANSPORT [3]. Solid angle of the separator is about 5.6 msr. The envelopes in horizontal (x) and vertical (y) directions are shown in the figure for the initial secondary-beam emittance of $\Delta x = \Delta y = \pm 1.5$ mm, $\Delta\theta_x = \Delta\theta_y = \pm 30$ mrad and $\Delta p/p = 0$. Only the horizontal focusing is achieved at F1, while F2 is doubly focussed. The magnification from F0 to F1 is 0.3 for x and those from F0 to F2 are 1.2 for x and 0.5 for y. At F2, the beam spot size can be in the order of 1 cm diameter which is small enough to perform experiments.

The momentum dispersion in the horizontal direction is also shown in Fig. 2 by a dashed line. It is seen that the dispersion at F1 (1.6 m) is determined by strengths of D1 and Q2 magnets. The horizontal width of F1 focal plane defines the maximum momentum acceptance of about $\pm 7.7\%$. The momentum resolving power at F1 is about 800.

The D2 magnet compensates the dispersion at F1 and gives a doubly achromatic focal plane at F2.

The magnetic spectrometer can rotate from $-5°$ to $60°$ around the F0 target position to select the scattering angle of reaction product. Usually, the spectrometer is set to $0°$ to collect forward focused ejectiles from a production reaction in inverse kinematics.

C. Wien Filter

A Wien filter (velocity filter) system has been assembled at the downstream side of the F2 focal plane of the magnetic separator to provide an additional particle-separation power. The construction has almost been finished and tuning of the high-voltage system and the beam transport test are now in progress.

The Wien filter line is 5 m long and consists of four quadrupole magnets (Q4, Q5, Q6 and Q7) and a velocity separation section (1.5 m long) between Q5 and Q6. The magnification from the entrance (F2) to exit (F3) is 1 for a typical operation. The maximum field gradients are 0.97 kG/cm for Q4 and Q7 and 1.8 kG/cm for Q5 and Q6. These are large enough to transport particles at the maximum magnetic rigidity of the magnetic spectrometer.

The velocity separation section consists of a dipole magnet with a 45-cm pole gap and two electrodes mounted in the gap space. The electrodes are set in parallel along the beam axis with an 8-cm gap. HIgh voltages ($\pm$200 kV maximum) is applied to the electrodes to make a horizontal electric field (50 kV/cm maximum), which is combined with the vertical magnetic field (2.9 kG maximum).

The $\vec{E} \times \vec{B}$ field produces velocity dispersion in horizontal direction. For particles with $A/q = 2$ at the energy of $E/A = 4.3$ MeV, the maximum velocity dispersion is expected to be 1.0 cm/% from F2 to F3. In this case, the velocity resolving power $v/\Delta v$ is 100 if the horizontal beam spot size is assumed to be 1.0 cm at F2.

All the elements of the Wien filter system are mounted on a movable frame which can be detached from the frame of magnetic spectrometer. When the Wien filter is unnecessary, the Wien filter frame can be moved aside to the parking position to make the experimental space wider around F2.

III. RI BEAMS PRODUCTION

Production yields of RI beams at CRIB have been estimated so far mainly for (p,n) reactions (see Fig. 3), which can produce proton-rich nuclei near the stable line. It is possible to use fusion reactions to produce nuclei little far from the stability line, and also to use (n,p)-type reactions like (d,2p) reactions to produce neutron-rich nuclei.

It is rather easy to obtain a secondary beam of 10^7-aps intensity by a (p,n) reaction of 10-mb cross section, with a 1-pμA primary beam and a 0.1-mg/cm^2 target. Due to the inverse kinematics, a heavy-ion RI beam produced by a (p,n) reaction is forward focused in the laboratory frame. The momentum and angular spread of the RI beam are roughly the same, namely $\Delta p/p \sim \Delta\theta$. These widths are in the order of $1/A$ or less and are comparable to the momentum acceptance and the solid angle of CRIB. Typically CRIB has several tens % of total acceptance for secondary particles produced by (p,n) reactions.

IV. RI BEAM SEPARATION

CRIB has three types of particle-separation power (#1–3). The first half of CRIB spectrometer F0-Q1-D1-Q2-F1 generates the momentum dispersion. A horizontal slit at F1 is used to select a region of magnetic rigidity for secondary particles of interest (#1 particle separation by $B\rho$). The primary beam is usually stopped at a beam stopper (Faraday cup) inside the D1 magnet.

Only with the particle separation by magnetic rigidity (F1 slit), there can be many background nuclides which have the same magnetic rigidity as the secondary beam. Light particles like p, d, α and so on are often produced by nuclear reactions and usually have large momentum distributions. Therefore, these light particles pass through the F1 slit and reach to F2. Scattering of the primary beam at the walls of beam pipes, the edge of the target holder and the inner walls of D1 magnet also produces background particles of the same nuclide as the primary beam.

To reduce background particles which pass through the F1 slit, one can install an energy degrader at the F1 plane, as often used for fragment separators [4,5]. The magnetic rigidity before the F1 degrader ($B\rho_1$) is defined by the F1 slit and independent of particle type, while the magnetic rigidity after the degrader ($B\rho_2$) depends on Z and velocity (thus A) because of energy loss. Thus, the second half of CRIB spectrometer F1-D2-M3-Q3-F2 with a horizontal slit at F2 serves as the second particle analyzer by $B\rho_2$. Among the group of nuclides which have the same $B\rho_1$, only nuclides with $A^{2.5}/Z^{1.5} \sim const.$ can go through the F2 slit (#2 particle separation by the energy-loss method).

Without the degrader, the second half of spectrometer compensates the momentum dispersion at F1 (D_1) and makes the F2 focal plane achromatic. The relation of dispersion compensation can be expressed as $D_1 + D_2/M_{x2} = 0$, where D_2 and M_{x2} are the dispersion and horizontal magnification, respectively, from F1 to F2. Inserting a flat plate degrader at F1 breaks the achromaticity from F0 to F2 because the energy dependence of energy loss changes the dispersion at F1. The dispersion at F1 with the flat degrader D_1' can be approximated by $D_1' \sim (1 - d/R)D_1$, where d is the degrader thickness and R is the range of particle in the degrader material. A degrader of wedge shape [4] may be used to keep the dispersion constant before and after the degrader ($D_1' = D_1$). Thickness of degrader is typically $d < 0.3R$. For low energy RI beams at $E/A < 10$ MeV, the degrader thickness is small (order of several mg/cm^2). It may be difficult to fabricate such a thin wedge degrader. Instead, one may use a curved-film degrader which has the same position dependence of effective thickness as the wedge shape.

It is also possible that one uses a simple flat degrader and modifies the dispersion at F1 instead, to keep the achromaticity at F2 [6]. For CRIB, we can adjust the dispersion before the F1 degrader by changing the strength of Q2 magnet. In this case, the dispersion should be set to $D_1 = -D_2/M_{x2}/(1 - d/R)$, so that the dispersion after the degrader becomes $D_1' = -D_2/M_{x2}$ and satisfies with the dispersion compensation relation.

As written in Sect. 2, the Wien filter system after F2 can be an additional section which provides a velocity dispersion (#3 particle-separation by velocity). This separation method

may be useful when the energy-degrader method is not effective enough, for example, in separating a proton-rich nuclide from the neighboring isotones.

V. EXPERIMENTAL PROJECT

One of the applications of the low-energy RI beams to nuclear physics is the study of resonant states in unstable nuclei, which are of interest with respect to exotic nuclear structure or nuclear astrophysics. The first experiment to be done at CRIB will be a search for resonant states in unstable nuclei via elastic scattering. Cross section of resonance elastic scattering near the threshold is very large if the partial width for the elastic channel is much larger than those of other reaction channels. Therefore the experiment can be performed easily with low-intensity RI beams. We are planning to measure ^{10}C+p (^{11}N), ^{12}N+p (^{13}O) and some other RI+p resonances in proton-rich nuclei. Data of those resonances is important to understand a hydrogen burning process at high temperature in metal deficient stars. Resonant states of unbound nuclei beyond the proton-drip line are interesting in conjunction with their mirror nuclei near the neutron-drip line.

An elastic scattering experiment can be performed in inverse kinematics with an RI beam and a proton target. In this situation, the center-of-mass energy and angle can be determined by measuring energy and angle of recoil proton in better resolution than by measuring those of the heavy ejectile. It is useful to apply the thick-target method [7,8], where the target thickness is chosen to be comparable to the range of incident beam in the target material. Due to large energy loss of the beam in the target, a wide range of the excitation function of elastic scattering can be measured at the same time. The recoil proton goes out from the target with very small energy-loss in the target and gives information on energy and angle of scattering. The proton is detected at forward angles in the laboratory frame. At a fixed angle, the proton energy spectrum has roughly the same shape as the excitation function $d\sigma/d\Omega(E)$ of elastic scattering. In the excitation function, a resonance can be identified as an interference pattern of potential scattering and resonance scattering. The center-of-mass

scattering angle for the forward-emitted recoil proton is nearly 180°, where the scattering amplitude for the Coulomb potential goes to minimum and the effect of resonance amplitude becomes more prominent.

An experimental setup for elastic resonance scattering will be constructed at CRIB F2. The setup consists of two PPACs for beam tagging, a thick CH_2 target and several sets of silicon detectors for the recoil proton. Each set of silicon detectors is capable of measuring ΔE-E, timing and position in order to identify proton and to determine its energy and scattering angle. If an RI beam of 10^5-aps intensity is used, enough number of elastic scattering events can be accumulated in a day.

VI. SUMMARY

The technique of low-energy RI beam production and separation by CRIB has been discussed in terms of production yield and transport optics. The CRIB system has been tested by using primary beams and test of RI beam production is now in progress. The RI beams produced by CRIB can be easily applied to the experiments of elastic resonance scattering. The first experiment will be performed in the year 2001.

REFERENCES

[1] T. Noro et al., RCNP Annual Report 1983, 173;

T. Yamagata et al., Phys. Rev. C39 (1989) 873.

[2] K. Sagara et al., Nucl. Instr. Meth. A257 (1987) 215.

[3] D.C. Carey et al., Fermilab-Pub-98-310.

[4] J.P. Dufour et al., Nucl. Instr. and Meth. A248 (1986) 267.

[5] T. Kubo et al., Nucl. Instr. and Meth. B70 (1992) 309.

[6] S. Mitsuoka et al., Nucl. Instr. and Meth. A372 (1996) 489.

[7] K.P. Artemov et al., Sov. J. Nucl. Phys. 52 (1990) 408.

[8] S. Kubono, Nucl. Phys. (2001) in press, and references therein.

FIGURES

FIG. 1. Layout of CRIB.

FIG. 2. Result of TRANSPORT calculation for CRIB. Solid lines are envelopes in x and y. Dashed line indicates the horizontal momentum dispersion.

FIG. 3. RI beams available at CRIB by (p,n) reactions in inverse kinematics. Intensity marked on each nuclide is for a primary beam of 1 pμA and a primary target of 0.1 mg/cm^2 and based on the experimental or calculated data of production cross section and the experimental data of ion source yield at RARF.

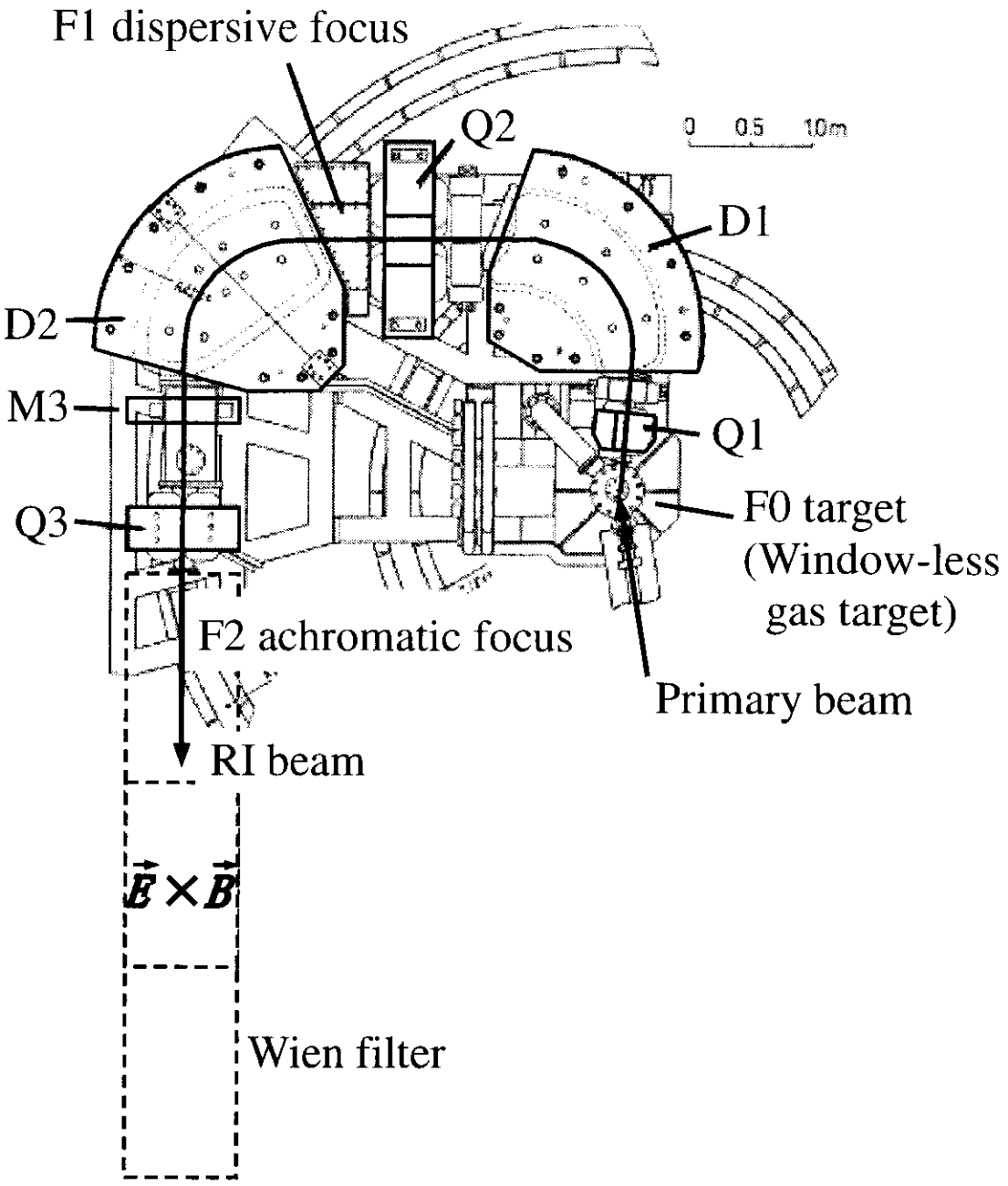
F1 dispersive focus
Q2
0 0.5 1.0m
D1
D2
M3
Q1
Q3
F0 target
(Window-less
gas target)
F2 achromatic focus
Primary beam
RI beam
$\vec{E} \times \vec{B}$
Wien filter

Figure 1

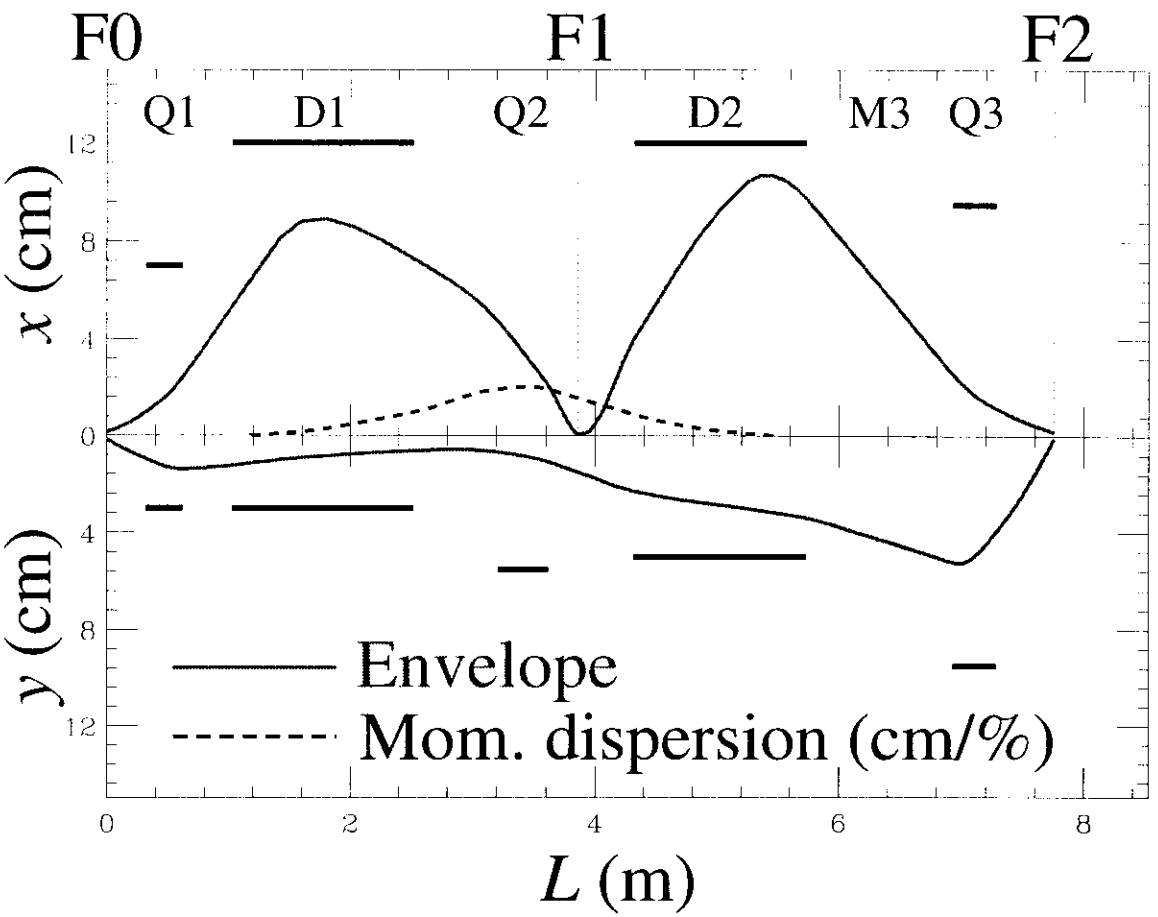
F0
F1
F2
Q1
D1
Q2
D2
M3
Q3
x (cm)
y (cm)
12
8
4
0
4
8
12
Envelope
Mom. dispersion (cm/%)
0
2
4
6
8
L (m)

Figure 2

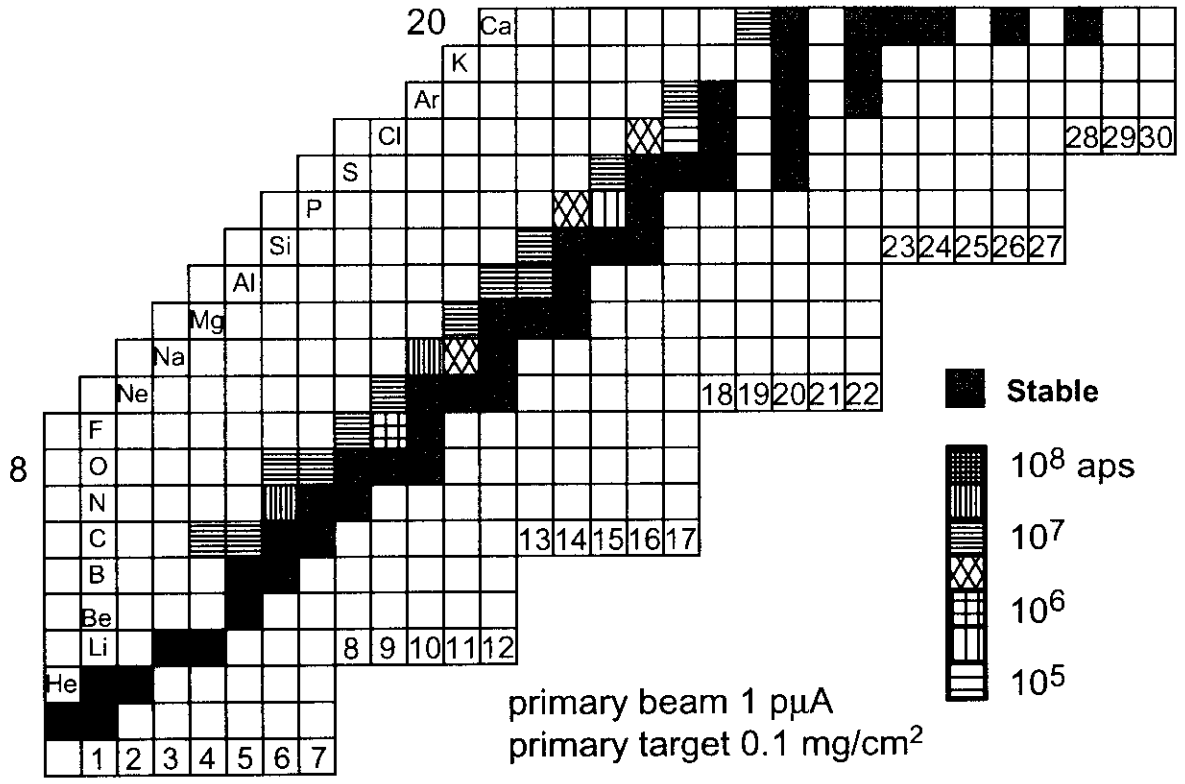
20
Ca
K
Ar
Cl
S
P
Si
Al
Mg
Na
Ne
F
O
N
C
B
Be
Li
He
8
1 2 3 4 5 6 7
8 9 10 11 12
13 14 15 16 17
18 19 20 21 22
23 24 25 26 27
28 29 30
Stable
10^8 aps
10^7
10^6
10^5
primary beam 1 pμA
primary target 0.1 mg/cm^2

Figure 3